Modeling analysis of port breakwater influence on water supply and drainage construction in coastal buildings

Aiping Song*, Wenbo Mao

School of Engineering, Yunnan University of Business Management, Kunming 650104, China, email: ynjjglxykyc@163.com (A. Song)

ABSTRACT

Wave cyclic load is transmitted to the water supply and drainage construction in the coastal buildings through the embankment and the sandy soil replacement layer. Cyclic dynamic stress is generated in the water supply and drainage construction of coastal buildings, which results in the weakening of undrained strength in the water supply and drainage construction of coastal buildings, severely affecting the bearing capacity of lattice steel sheet pile breakwater. Combined with the engineering numerical examples, based on the dynamic finite element method, an analysis model for the water supply and drainage construction of coastal buildings considering the port breakwater is established to study and the maximum pore pressure growth law of the water supply and drainage construction in the coastal buildings under the cyclic load as well as the weakening characteristics of undrained shear strength. The modeling and analysis method for the influence on the water supply and drainage construction of coastal buildings is established to analyze the failure mode, stability, and settlement deformation characteristics of the water supply and drainage construction in the coastal buildings. The results show that the maximum pore water pressure is mainly distributed in the soft soil layer around the lattice, and there is a significant weakening in the undrained shear strength at the bottom of the main and sub-lattice and part of the pile-soil contact area. Considering that due to the cyclic weakening effect of the water supply and drainage construction in the coastal buildings, the safety factor of stability is significantly reduced in the water supply and drainage construction of the coastal buildings, it is recommended that the influence of cyclic weakening effect of the water supply and drainage construction in the coastal buildings on the stability of lattice steel sheet pile breakwater should be taken into consideration in the practical engineering.

Keywords: Water supply and drainage construction of coastal buildings; Lattice steel sheet pile; Maximum pore water pressure; Undrained shear strength; Stability

1. Introduction

Port breakwater is a structural type of hydraulic structure suitable for the water supply and drainage construction of coastal buildings, where the closed lattice is formed by straight or curved steel sheet piles, and the lattice is filled with gravel aggregate. As its construction is quick and convenient, it is suitable for offshore construction [1–4]. Therefore, it has an excellent application prospect in hydraulic structures such as breakwaters, seawalls, and artificial island cofferdams in deep water conditions and so on. Some studies have been carried out on the port breakwaters previously. Shell units and articulated connectors are used to simulate the relative rotation between the steel sheet pile and the adjacent sheet piles to establish a finite element numerical model for studying the stability of the lattice steel sheet pile breakwater under the wave static load [5–8], the stress distribution characteristics of the sheet pile lock and so on [9–14]. Comparative analysis is carried out on the stability of lattice steel sheet pile breakwater and the distribution characteristics of sheet pile hoop stress under

* Corresponding author.

different modeling methods to provide suggestions for the application of the numerical modeling method of lattice steel sheet pile breakwater in the practical engineering [15–18]. Although the static characteristics of port breakwater have been studied, strictly speaking, as the wave load is a dynamic effect, the static finite element numerical model cannot reflect the influence characteristics of the breakwater reasonably [19–25].

The influencing model for the water supply and drainage construction of coastal buildings is established for analysis, and numerical development is used to implement the dynamic finite element method for the calculation of undrained shear strength in the water supply and drainage construction of coastal buildings. The dynamic finite element method has few parameters and is simple and easy to use, which can reasonably simulate the cyclic weakening characteristics of undrained shear strength in the water supply and drainage construction of coastal buildings. Therefore, combined with the engineering numerical example, the dynamic finite element method and based on the calculation of the cyclic weakening characteristics of undrained shear strength in the water supply and drainage construction of coastal buildings, an analysis model for the water supply and drainage construction of coastal buildings considering the port breakwater is established to study the maximum pore pressure increase law under the cyclic load effect of the water supply and drainage construction in coastal buildings as well as the influencing characteristics such as the cyclic weakening characteristics of undrained shear strength in the water supply and drainage construction. The modeling analysis method for the influence of water supply and drainage construction of coastal buildings considering the cyclic weakening characteristics of undrained shear strength in the water supply and drainage construction of coastal buildings is established to analyze the failure mode, stability characteristics, and deformation characteristics of the water supply and drainage construction in coastal buildings under cyclic loading effect, to provide a basis for the practical engineering design.

2. Project overview and construction impact model analysis

2.1. Project overview

The design for the lattice artificial island cofferdam of the harbor breakwater is calculated. The diameter of the main lattice of the port breakwater is 24.82 m, the radius of the sub-lattice is 7.32 m, and the center spacing of the main lattice chamber is 27.91 m. The plan and section of the structure are shown in Figs. 1 and 2, respectively. As it is a temporary structure, the calculation conditions adopt the high-water level in 10 years and the wave in 10 years. Among them, the hydrological conditions are shown in Table 1. The design wave conditions are shown in Table 2, and the wave force is calculated accordingly. The calculation parameters of the soil layers are shown in Table 3. Under the effect of cyclic wave loading, the phenomenon of undrained shear strength weakening occurs in the water supply and drainage construction of the coastal buildings in the silty clay layer and the silty clay sand layer.
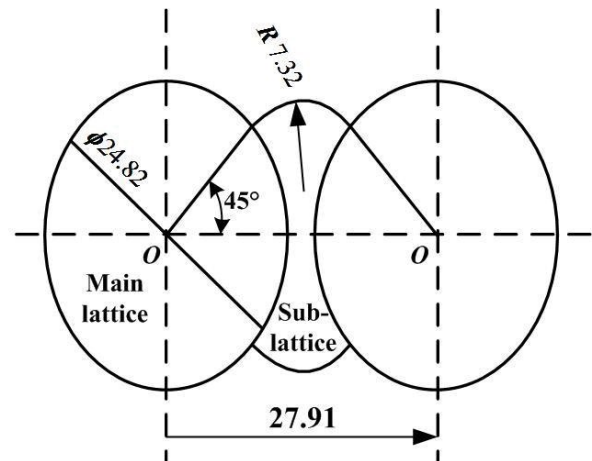

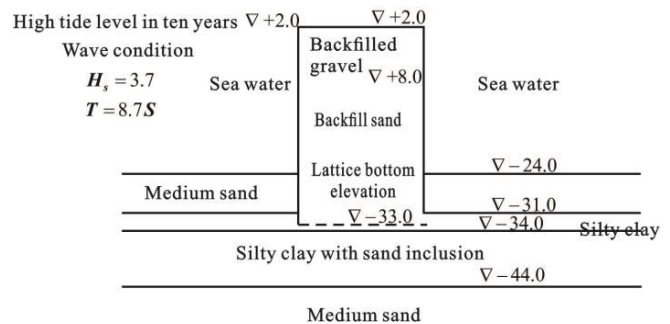Fig. 1. Floor plan of the harbor breakwater (unit: m).

Fig. 2. Sectional view of the port breakwater (unit: m).

Table 1
Water level in the engineering design

Recurrence period, a	10
High water level, m	2.0
Low water level, m	−1.0
High tide level, m	1.7
Low tide level, m	−0.8

Table 2
Engineering wave conditions

Direction	S
H_1, %	3.7
Period, s	8.7

2.2. Analysis model for the influence of water supply and drainage construction in coastal buildings

The contact setting and mesh division of the coastal building water supply and drainage construction influence analysis model are the same as the static model. As the wave load is a dynamic action, the dynamic analysis steps shall be set in the analysis steps. In the actual engineering,

Table 3
Soil parameters at different soil layers

Soil layer	Elevation/m	Unit weight of soil/(kN/m³)	Buoyant gravity density/(kN/m³)	Angle of internal friction/(°)	Cohesive strength/kPa
Backfill gravel	+2–8	17.00	11.00	39.0	0.0
Backfill sand	−8–33	18.00	9.50	32.0	0.0
Medium coarse sand (densely packed)	−24–31	18.00	9.50	32.0	0.0
Silty clay	−31–34	18.60	8.60	20.4	17.2
Silty clay with sand inclusion	−34–44	18.30	8.30	22.4	16.8
Medium sand	−44–80	20.17	10.17	35.8	5.0

the wave power acting on the breakwater is highly complicated. In order to make a comparison with the static analysis model, it is assumed in this paper that the wave force acting on the breakwater structure is a regular wave with a sinusoidal variation and that the corresponding wave force at the peak is the same as the wave suction value corresponding to the trough. Hence, the following equation can be used to express the basic verification polynomial matrix corresponding to the water supply and drainage construction impact model of coastal buildings:

$$h(x) = \begin{bmatrix} h_{1,1}(x) & h_{1,2}(x) & \cdots & h_{1,n}(x) \\ \vdots & \vdots & \ddots & \vdots \\ h_{n-k,1}(x) & h_{n-k,2}(x) & \cdots & h_{n-k,n}(x) \end{bmatrix}_{(n-k)\times n} \quad (1)$$

$$h_{i,j}(x) = h_{i,j}^0 + h_{i,j}^1 x + \cdots + h_{i,j}^K x^K, i = 1,\cdots,n-k; j = 1,\cdots,n \quad (2)$$

In the above Eqs. (1) and (2):

$$K = \max_{i,j}\left\{\deg\left(h_{i,j}(x)\right) \middle| i = 1,\cdots,n-k; j = 1,\cdots,n\right\} \quad (3)$$

In the above Eq. (3), K stands for the constraint degree of the port breakwater. The row vector coefficient $h(x)$ is extracted to obtain the basic frame check sequence:

$$h_i = \left[h_{i,1}^0,\cdots,h_{i,1}^K,h_{i,2}^0,\cdots,h_{i,2}^K,\cdots,h_{i,n}^0,\cdots,h_{i,n}^K\right], i = 1,\cdots,n-k. \quad (4)$$

The coding matrix C can be obtained by using the data interaction application method between the water supply and drainage construction models of the coastal buildings, and the verification relationship between C and the sequence in the above Eq. (1) is as the following:

$$C = \begin{bmatrix} c_1 & \cdots & c_n & \cdots & c_{Kn+1} & \cdots & c_{(K+1)n} \\ c_{n+1} & \cdots & c_{2n} & \cdots & c_{(K+1)n+1} & \cdots & c_{(K+2)n} \\ \vdots & \ddots & \vdots & \ddots & \vdots & \ddots & \vdots \\ c_{(N-1)n+1} & \cdots & c_{Nn} & \cdots & c_{(K+N-1)n+1} & \cdots & c_{(K+N)n} \end{bmatrix} \quad (5)$$

$$C \cdot h_i^T = 0, i = 1,\cdots,n-k. \quad (6)$$

But for the matrix G thus generated, the verification relationship with the basic verification sequence can be expressed as the following:

$$C \cdot h_i^T = 0. \quad (7)$$

In summary, the problem of data interaction between the water supply and drainage construction influence models of coastal buildings can be described as the following: Pursuant to a certain law, the coding matrix can be established by using the received sequence. At this time, the basic verification sequence to be solved is the solution vector obtained by solving the Eq. (6). Similarly, the basic generator matrix can be obtained by solving the Eq. (7).

The stress-strain relationship of sand and gravel follows the basic verification polynomial matrix, and the dynamic finite element method is adopted for the soft soil layer to consider the undrained shear strength weakening phenomenon. It should be noted that the water supply and drainage construction of different coastal buildings will present different strength reduction characteristics under the effect of cyclic loading. In view of the lack of experimental data, the undrained shear strength reduction law is applied in this paper to the silty clay layer and silty clay sand layer in the numerical example in the literature, to provide an idea and basis for the practical engineering design.

3. Characteristics of the influence of water supply and drainage construction in coastal buildings

3.1. Distribution law of maximum pore water pressure

The increase of pore water pressure inside the soil can result in the weakening of the undrained shear strength in the soft soil layer. Figs. 3 and 4 show the distribution cloud diagram of the maximum pore water pressure in the soft soil below the main lattice chamber (the central axis section along the direction of the wave force action) and the sub-lattice (the central axis section along the direction of the wave force action) under different wave force loading factors. As the cyclic stress is very small, the soft boundary soil does not generate pore water pressure basically. The pore water pressure is mainly distributed in the soft soil around the lattice, and the maximum pore water pressure is generally shown in the middle of the soft soil layer below the lattice. This is due to the static deviatoric stress generated by the filling of the lattice and the cyclic stress transmitted
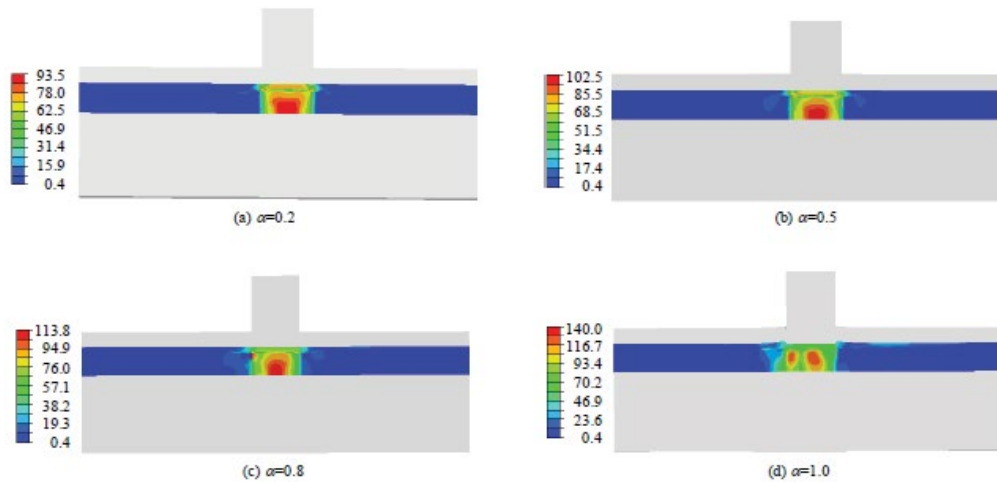
Fig. 3. Cloud diagrams of the maximum pore water pressure distribution under the main lattice chamber based on different wave force loading factors (a) α = 0.2, (b) α = 0.5, (c) α = 0.8, and (d) α = 1.0 (unit of measurement: kPa).
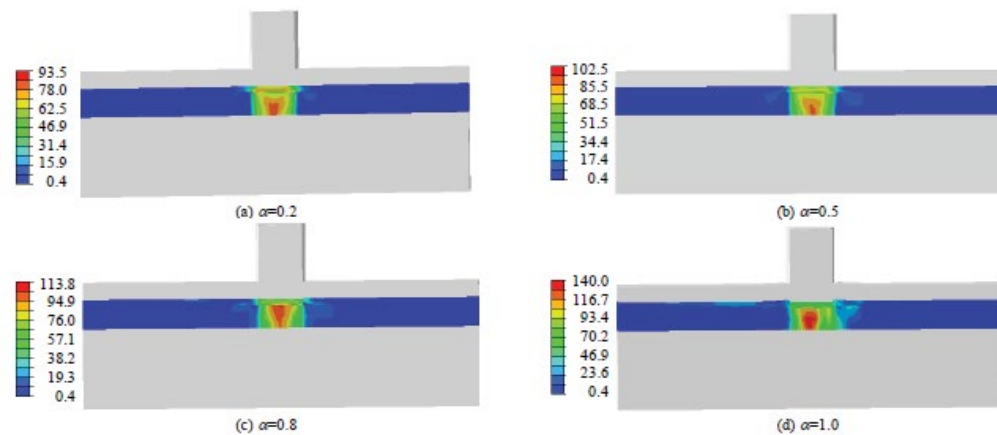

Fig. 4. Cloud diagrams of the maximum pore water pressure distribution under the sub-lattice chamber based on different wave force loading factors (a) α = 0.2, (b) α = 0.5, (c) α = 0.8, and (d) α = 1.0 (unit of measurement: kPa).

to the soft soil through the lattice and the surrounding solid pressure of the soil with the linear increase of the soil depth. Due to the joint action, the maximum cyclic water pressure will also occur in some pile-soil contact parts due to the large cyclic stress transmitted from the lattice to the soft soil. The main lattice chamber is the main bearing body, and the soft soil below the main lattice chamber is subject to greater static deviator stress and cyclic stress than that of the sub-lattice. Hence, the pore water pressure distribution cloud area of the soft soil layer below the main chamber is larger than that of the sub-lattice as the wave force loading coefficient α increases. The pore water pressure distribution cloud map area increases. Water nip pressure increase with increasing loading cycles, after a certain number of cycles in the pore water pressure stabilized, contours of the area remain substantially unchanged.

3.2. Distribution law of undrained shear strength in the soft soil layer

Figs. 5 and 6 show the distribution cloud diagram of the undrained shear strength at the soft soil layer under different wave cyclic stress levels and cyclic loading times below the main lattice chamber (the axial section along the direction of the wave force) and the secondary silo (the section along the central axis of the wave force). There is basically no weakening of the undrained shear strength at the boundary foundation soil, and the undrained shear strength of the soil presents a linear distribution with the depth of the soil. Under the joint action of the static deviator and cyclic load of the backfilled soil in the U lattice, the undrained intensity distribution presents a bowl-shaped distribution in the cloud diagram, which indicates that the soft soil layer in the lower part of the lattice body is prone to insufficient bearing capacity and that the undrained shear strength of the soft soil at the bottom of the main and sub-lattice chamber is significantly weakened. The undrained shear strength value of some pile-soil contact parts will also be significantly reduced. As the force loading coefficient α and the number of cyclic loadings N increase, and the weakened area is increased significantly. However, after a certain number of cycles, the weakened area remains basically unchanged.
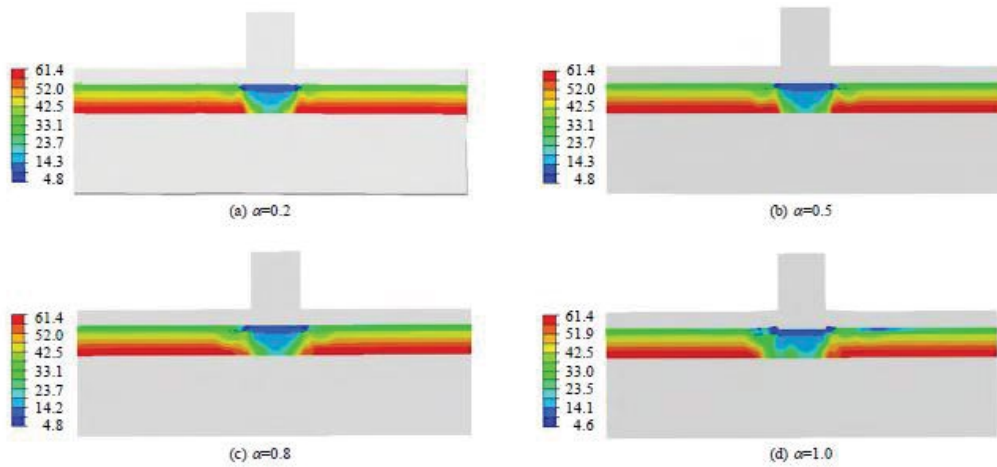
Fig. 5. Cloud diagrams of the undrained shear strength distribution under the main lattice chamber based on different wave force loading factors (a) α = 0.2, (b) α = 0.5, (c) α = 0.8, and (d) α = 1.0 (unit of measurement: kPa).
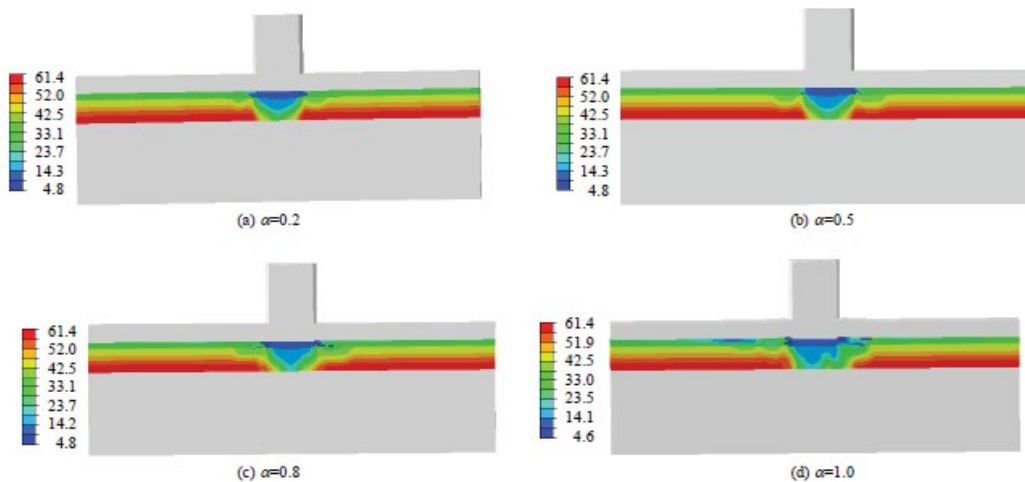

Fig. 6. Cloud diagram of the undrained shear strength distribution under the sub-lattice chamber based on different wave force loading factors (a) α = 0.2, (b) α = 0.5, (c) α = 0.8, and (d) α = 1.0 (unit of measurement: kPa).

4. Experiment and result analysis

4.1. Failure mode

The structural displacement is relatively sensitive to the magnitude of the wave force acting on the structure. Figs. 7 and 8 show the displacement cloud diagrams under different wave force loading coefficients and wave load cycles. When the wave cyclic stress level is relatively low, no structural displacement accumulation is generated in the lattice. When the wave cyclic stress level is relatively high, the lattice body rotates around a certain point at the bottom of the structure. When the cyclic stress level continues to increase, in the initial cycle phase, the rotation of lattice steel plate pile body occurs around a certain point at the bottom of the structure; with the increase in the number of cyclic loadings, the wave cyclic load leads to extrusion, tension and friction on the surrounding solid body around the lattice body, causing soil arches in the foundation soil. At the same time, due to the construction of water supply and drainage in coastal buildings, the drainage intensity is weakened, the granular body sinks into the coastal building water supply and drainage construction and squeezes the soil at the bottom of the lattice body, and the cumulative plastic deformation of the bottom and surrounding soft soil occurs, hence the occurrence of punching and shearing damage in the foundation soil. The failure mode of water supply and drainage construction in the coastal buildings is insufficient for the bearing capacity of the foundation. The analysis results of the static construction influence model show the rotation instability of a point around the bottom of the lattice, and the calculation results in the two cases are significantly different.

4.2. Stability analysis

Considering the weakening of the construction and drainage of coastal buildings, the failure mode of the lattice steel sheet pile breakwater is insufficient for the bearing
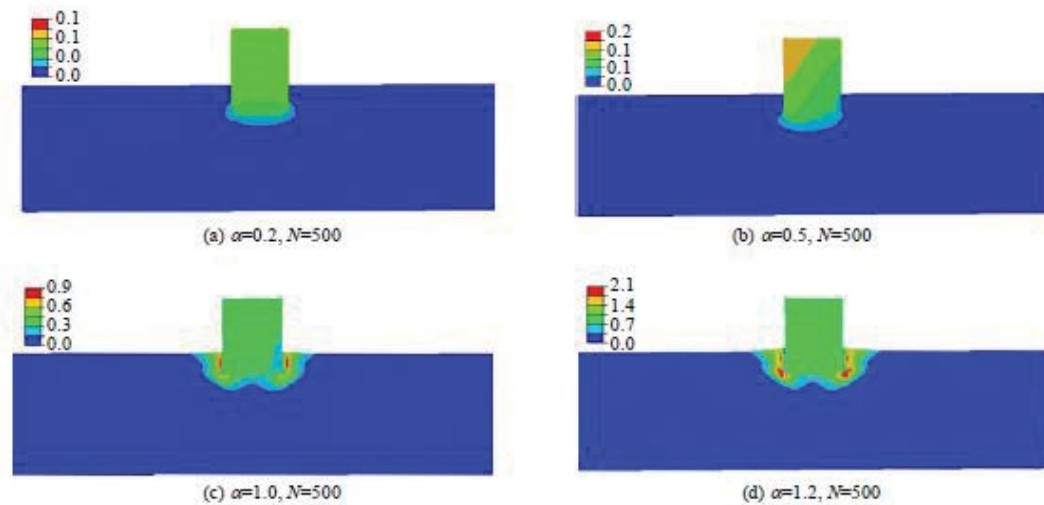
Fig. 7. Cloud diagrams of the displacement distribution of the breakwater under different wave force loading factors (a) $\alpha = 0.2$, $N = 500$; (b) $\alpha = 0.5$, $N = 500$; (c) $\alpha = 1.0$, $N = 500$; and (d) $\alpha = 1.2$, $N = 500$ (unit of measurement: m).
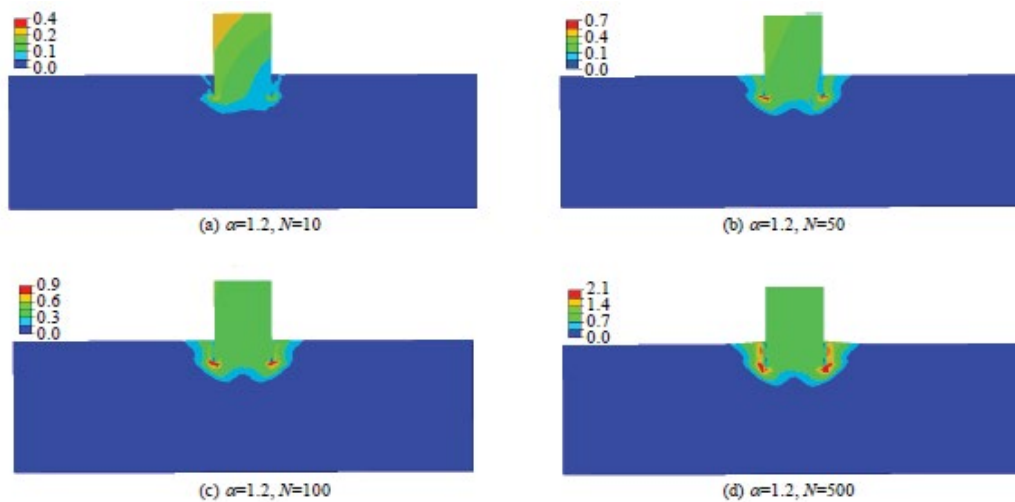

Fig. 8. Cloud diagrams of the displacement distribution of the breakwater under different cyclic counts (a) $\alpha = 1.2$, $N = 10$; (b) $\alpha = 1.2$, $N = 50$; (c) $\alpha = 1.2$, $N = 100$; and (d) $\alpha = 1.2$, $N = 500$ (unit of measurement: m).

capacity of the foundation. In reference to the box-type foundation dynamic stability analysis method, the dynamic stability modeling analysis method of the lattice steel sheet pile breakwater is as the following:

- Apply wave cyclic load, the wave force loading coefficient starts from 0 and increases by 0.1 step by step, and 500 times are taken as the number of wave load cycles to carry out calculation according to the "dynamic finite element method;"
- Extract the wave force amplitude of each level in the finite element result and the corresponding maximum settlement of the lattice body after the corresponding cyclic load and then plot the wave force-lattice settlement curve. The curve at this point is actually the breakwater load-displacement response envelope curve.

- Based on the ideal plastic failure criterion, the safety factor K of shear failure of water supply and drainage construction in coastal buildings can be obtained.

As shown in Fig. 9, when the wave force loading coefficient is relatively small, the wave force-lattice settlement curve changes substantially linearly. When the wave force loading coefficient is relatively large, the wave force-lattice settlement curve presents a significant inflection point, indicating the coastal building water supply and drainage starts to show large plastic deformation. Considering that in the long-term circulation weakening of the coastal construction water supply and drainage construction, the safety factor of lattice steel sheet pile breakwater stability is 1.3, and the structure under the wave force design is safe.

4.3. Analysis of lattice settlement

Under the undulating cyclic load, the undrained shear strength of the coastal water supply and drainage construction is weakened, resulting in insufficient foundation bearing capacity and large settlement of the lattice steel sheet pile breakwater. Fig. 10 shows the wave force-lattice settlement curve calculated by different calculation methods for the same design wave force using the wave force loading coefficient method. Considering the weakening effect of the undrained shear strength of the coastal water supply and drainage construction, the calculated value of the static method is significantly larger than that calculated by the dynamic finite element method and the quasi-static method. The lattice settlement calculated by the meta-method is significantly larger than that calculated by the pseudo-static method. The main reasons are as the following: (1) Compared with the pseudo-static method, the dynamic finite element method can reflect the cumulative effect of plastic deformation of the soil under the action of wave circulation; (2) The wave cyclic load is transferred to the foundation through the lattice body and generates the cyclic stress in the water supply and drainage construction of the coastal buildings. The cyclic stress distribution of the soft soil layer is uneven, where the upper cyclic stress value is significantly larger than the lower part of the soft soil layer, and the quasi-static method passes through the

Fig. 9. Wave force-lattice settlement curve.

Fig. 10. Wave force-lattice settlement displacement curve based on different calculation methods.

soil unit in the middle of the soft soil layer. The stress reduction factor is used to calculate the strength reduction factor, which underestimates the influence of the weakening of the soft upper soil on the settlement. The dynamic finite element method is used to show the variation law of the strength reduction factor in each soil unit at the soft soil layer with the cyclic stress level and the number of cyclic loading, which can reflect the unevenness of the weakening in the undrained shear strength at the soft soil layer. The settlement thus calculated is larger than that calculated according to the static method.

5. Conclusions

The wave cyclic loading effect causes the accumulation of significant plastic deformation in the water supply and drainage construction of coastal buildings and leads to the weakening phenomenon of an undrained shear strength cycle, which can affect the stability of the lattice steel sheet pile breakwater. The dynamic finite element method is applied to analyze the pore water pressure to increase law in the water supply and drainage construction of coastal buildings and the weakening characteristics of undrained shear strength. In addition, the failure mode, stability, and settlement deformation characteristics of the lattice steel sheet pile breakwater in the water supply and drainage construction of coastal buildings as well as the influence of sheet pile depth in the earth on the stability of water supply and drainage construction in the coastal buildings. The pore water pressure is mainly distributed in the soft soil layer around the lattice body. The maximum pore water pressure generally occurs in the middle of the soft soil layer below the lattice body. The maximum pore water pressure can also occur in some of the pile-soil contact parts. The area of the cloud diagram for the pore water pressure distribution in the soft soil layer below the main lattice chamber is slightly larger than that of the sub-lattice chamber. The weakening phenomenon of undrained shear strength in the water supply and drainage construction of coastal buildings has a significant influence on the stability and failure mode of the water supply and drainage construction in the coastal buildings. The failure mode of lattice steel sheet pile breakwater is the insufficient bearing capacity of the foundation, which is significantly different from the static analysis method. The stability safety factor of the water supply and drainage construction in coastal buildings is significantly reduced compared with that when the weakening of the water supply and drainage construction cycle in coastal buildings is not taken into consideration. The settlement displacement calculated according to the dynamic finite element method and the pseudo-static method is significantly increased in the computed value compared with that calculated according to the static method. The dynamic finite element method can reflect the dynamic characteristics of the structure and the weakening phenomenon of the undrained shear strength in the water supply and drainage construction of coastal buildings. The calculated settlement displacement of the lattice is higher than that calculated according to the pseudo-static method. In practical engineering, the stability of the lattice steel sheet pile can be increased by increasing the depth of sheet pile in the earth.
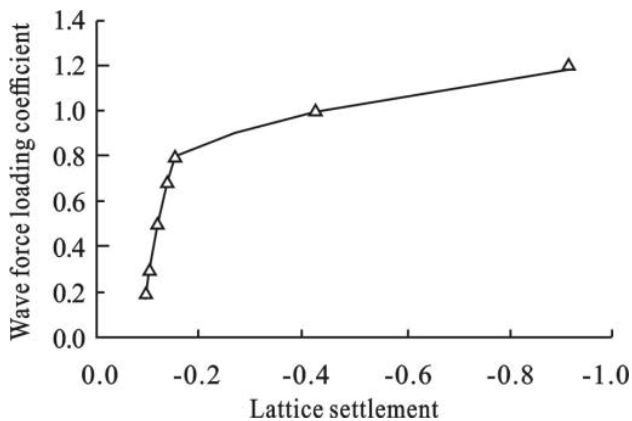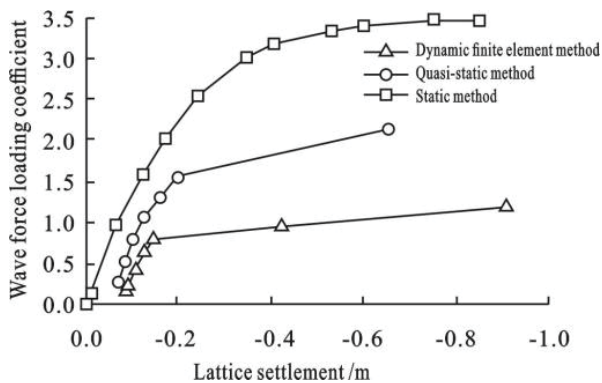
References

[1] P.S. Pauw, E.S. Van Baaren, M. Visser, P.G.B. De Louw, G.H.P.O. Essink, Increasing a freshwater lens below a creek ridge using a controlled artificial recharge and drainage system: a case study in the Netherlands, Hydrogeol. J., 23 (2015) 1415–1430.

[2] J.J. Meisinger, R.E. Palmer, D.J. Timlin, Effects of tillage practices on drainage and nitrate leaching from winter wheat in the Northern Atlantic coastal-plain USA, Soil Tillage Res., 151 (2015) 18–27.

[3] M.L. Gaytan-Herrera, E. Cuna-Perez, P. Ramirez-Garcia, Annual phytoplankton dynamics in la antigua river, mexico, J. Environ. Biol., 38 (2017) 1197–1203.

[4] A. Kylili, P.A. Fokaides, A. Ioannides, S. Kalogirou, Environmental assessment of solar thermal systems for the industrial sector, J. Cleaner Prod., 176 (2018) 99–109.

[5] L.M.J. Millani, S. Judith, V.T. Pablo, B. Peter, Impact of drainage and soil hydrology on sources and degradation of organic matter in tropical coastal podzols, Geoderma, 330 (2018) 79–90.

[6] S. Issaka, M.A. Ashraf, Impact of soil erosion and degradation on water quality: a review, Geol. Ecol. Landscapes, 1 (2017) 1–11, doi: 10.1080/24749508.2017.1301053.

[7] R.J. Yao, J.S. Yang, T.J. Zhang, L.Z. Hong, M.W. Wang, S.P. Yu, Studies on soil water and salt balances and scenarios simulation using saltmod in a coastal reclaimed farming area of eastern china, Agric. Water Manage, 131 (2014) 115–123.

[8] S.B. Reid, D.H. Goodman, Pacific lamprey in coastal drainages of California: occupancy patterns and contraction of the southern range, Trans. Am. Fish. Soc., 145 (2016) 703–711.

[9] T.W. Gallien, B.F. Sanders, R.E. Flick, Urban coastal flood prediction: integrating wave overtopping, flood defenses and drainage, Coast Eng., 91 (2014) 18–28.

[10] A.M. Foyle, Groundwater flux as a determinant of coastal-zone upland loss: a case study from the Pennsylvania coast of Lake Erie, USA, Environ. Earth Sci., 71 (2014) 4565–4578.

[11] J.P. Beamer, D.F. Hill, A. Arendt, G.E. Liston, High-resolution modeling of coastal freshwater discharge and glacier mass balance in the Gulf of Alaska watershed, Water Resour. Res., 52 (2016) 3888–3909.

[12] U. Mandal, S. Sahoo, S.B. Munusamy, A. Dhar, S.N. Panda, A. Kar, Delineation of groundwater potential zones of coastal groundwater basin using multi-criteria decision making technique, Water Resour. Res., 30 (2016) 4293–4310.

[13] F. Fikriah, Y. Kamaruzzaman, M. Mohd Fuad, A. Azman, Assessment of trace metals using chemometric analysis in Kuantan River, East Coast Malaysia, J. Clean WAS, 3 (2019) 01–04.

[14] R.M. Fuentes Rivas, G. Santacruz De Leon, J.A. Ramos Leal, J. Moran Ramirez, F. Martin Romero, Characterization of dissolved organic matter in an agricultural wastewater-irrigated soil, in semi arid Mexico, Rev. Int. Contam. Ambiental, 33 (2017) 575–590.

[15] M. Antonellini, D.M. Allen, P.N. Mollema, D. Capo, N. Greggio, Groundwater freshening following coastal progradation and land reclamation of the Po Plain, Italy, Hydrogeol. J., 23 (2015) 1009–1026.

[16] N.T. Schock, B.A. Murry, D.G. Uzarski, Impacts of agricultural drainage outlets on great lakes coastal wetlands, Wetlands, 34 (2014) 297–307.

[17] T.W. Appelboom, G.M. Chescheir, R.W. Skaggs, J.W. Gilliam, D.M. Amatya, Nitrogen balance for a plantation forest drainage canal on the North Carolina Coastal Plain, Am. Soc. Agric. Biol. Eng., 51 (2014) 1215–1233.

[18] P. Xin, X. Yu, C. Lu, L. Li, Effects of macro-pores on water flow in coastal subsurface drainage systems. Adv. Water Resour., 87 (2016) 56–67.

[19] C. Authemayou, K. Pedoja, A. Heddar, S. Molliex, A. Boudiaf, B. Ghaleb, Coastal uplift west of algiers (algeria): pre- and post-messinian sequences of marine terraces and rasas and their associated drainage pattern, Int. J. Earth Sci., 106 (2017) 19–41.

[20] S.Z. Czobel, L. Horvath, P. Posa, J. Schellenberger, J. Skutai, O. Szirmai, Dependence of CO_2 flux on the key abiotic and biotic parameters in semi-natural grasslands either traditionally grazed or excluded from grazing, Appl. Ecol. Environ. Res., 15 (2017) 15–23.

[21] V. Havrysh, V. Nitsenko, Y. Bilan, D. Streimikiene, Assessment of optimal location for a centralized biogas upgrading facility, Energy Environ., 30 (2019) 462–480.

[22] R. Rodeano, Engineering geological investigation on karam-bunai-lok bunuq landslides, Kota Kinabalu, Sabah, Malaysian J. Geosci., 3 (2019) 01–06.

[23] M.O. Eyankware, Hydrogeochemical assessment of chemical composition of groundwater; a case study of the Aptian-Albian aquifer within sedimentary basin (Nigeria), Water Conserv. Manage., 3 (2019) 01–07.

[24] H. Diego, M. Zen, M. Karen, Analysing trade-offs in management decision-making between ecosystem services, biodiversity conservation, and commodity production in the Peruvian Amazon National Reserve, Environ. Ecosyst. Sci., 3 (2019) 01–08.

[25] C.R. Mattheus, A.B. Rodriguez, Controls on lower-coastal-plain valley morphology and fill architecture, J Sediment Res., 84 (2014) 314–325.